frontiers in Energy Research

ORIGINAL RESEARCH
published: 07 December 2020
doi: 10.3389/fenrg.2020.573267

Process Simulation and Economic Analysis of Pre-combustion CO_2 Capture With Deep Eutectic Solvents

*Kun Xin, Mahmoud Hashish, Ivo Roghair and Martin van Sint Annaland**

Department of Chemical Engineering and Chemistry, Chemical Process Intensification, Eindhoven University of Technology, Eindhoven, Netherlands

The purpose of this paper is to identify firstly the most important solvent characteristics in the CO_2 capture process and secondly to determine how they contribute to the total cost of CO_2 separation and analyze the economic feasibility of current deep eutectic solvents (DESs) in literature. A rate-based modeling approach was adopted to simulate pre-combustion CO_2 capture. The effects of the flow model and the number of segments were investigated for the Selexol process. Different mass transfer correlations due to Bravo et al. (1985), Billet and Schultes (1993) and Hanley and Chen (2012) were adopted for the rate-based models and compared with the equilibrium modelling approach. Subsequently, property and process models were developed for a mixture of decanoic acid and menthol, in equal quantities. A physical property study was conducted with this DES. The CO_2 solubility is found to be very important in all rate-based models, as expected, but properties such as the surface tension, thermal conductivity, heat capacity and volatility had a minor influence on the absorption performance. The solvent viscosity strongly affects the mass transfer rate when using the Hanley and Chen (2012) correlations, whereas it plays only a small role in the other two sets of correlations. Using a high CO_2 solubility as criterion, two mixtures of allyl triphenylphosphonium bromide (ATPPB) and diethylene glycol (DEG) were screened out from literature. The conventional Selexol process was set as the benchmark for the evaluation of the performances of these DESs. The optimum capture cost for Selexol process is 27.22, 26.66 and 30.84 $\$_{2018}$/tonne CO_2 for the adopted correlations, respectively. When employing two of the three studied mass transfer correlations, the estimated process costs for a capture process using this DES can be similar to the costs of the Selexol process. However, when the liquid viscosity strongly affects the mass transfer rate, as is the case when using the Hanley and Chen (2012) correlations, the Selexol process remains more economical. This strongly indicates the need for further experimental and modelling studies on mass transfer rates in absorption columns (with higher viscosity liquids) to help directing the development of suitable DESs for pre-combustion CO_2 capture.

Keywords: pre-combustion CO_2 capture, property study, deep eutectic solvent, rate-based model, capture cost, selexol process

OPEN ACCESS

Edited by:
Sicong Tian,
Macquarie University, Australia

Reviewed by:
Hannu-Petteri Mattila,
Independent Researcher,
Parainen, Finland
Yacine Benguerba,
University Ferhat Abbas of Setif,
Algeria

****Correspondence:***
Martin van Sint Annaland
m.v.sintannaland@tue.nl

Specialty section:
This article was submitted to Carbon Capture, Storage, and Utilization, a section of the journal Frontiers in Energy Research

Received: *16 June 2020*
Accepted: *27 October 2020*
Published: *07 December 2020*

Citation:
Xin K, Hashish M, Roghair I and van Sint Annaland M (2020) Process Simulation and Economic Analysis of Pre-combustion CO_2 Capture With Deep Eutectic Solvents. Front. Energy Res. 8:573267. doi: 10.3389/fenrg.2020.573267

INTRODUCTION

In order to control and reduce anthropogenic greenhouse gas emissions, especially CO_2, CO_2 capture from fossil fuel power plants is getting great attention. Currently, there are four major technical routes to capture CO_2 from power plants, viz. pre-combustion, oxy-fuel, post-combustion and chemical looping combustion. Pre-combustion CO_2 capture is associated with the integrated gasification combined cycle (IGCC) and has been considered as a feasible way by separating CO_2 from H_2. Since the CO_2 partial pressure in the flue gas is relatively high, it is quite common to use physical absorption for the CO_2 capture (Ban et al., 2014). Among the various technologies for CO_2 capture, some of the physical absorption based technologies are relatively mature (Burr and Lyddon, 2008). The Selexol process is a bulk carbon dioxide absorption technique that applies a mixture of dimethyl ether polyethylene glycols (DEPG) as solvent, with formula $CH_3O(C_2H_4O)_nCH_3$, where n ranges from 2 to 9.

Many of the solvents used for CO_2 capture evaporate into the atmosphere with harmful effects on the environment and human health. Several novel solvents have been developed to reduce these effects. Ionic liquids (ILs) are considered as promising solvents because of their benign properties such as negligible vapor pressures, low melting points and high thermal stabilities. In addition, ILs are designable solvents, which makes it possible to tailor the physicochemical properties of the IL for the aimed application. However, traditional ILs suffer from the disadvantages of high production costs and toxicity. At the beginning of this century, a new generation of solvents, namely deep eutectic solvents (DESs), have emerged (Garcia et al., 2015). DESs share some of the promising characteristics of ILs, such as a low melting point and extremely low volatility. They can also be designed to show non-flammability, non-toxicity, water-compatibility an biodegradability (Sarmad et al., 2017). In addition, DESs can be very easily prepared, have 100% reaction mass efficiency and zero emission during their synthesis.

Specific physico-chemical properties of an absorbent can be tuned by modifying the molecular structures, changing the solvent type or mixing with other solvents. Whatever the solvent type or its composition, the physico-chemical and thermodynamic properties of the absorbent can be represented by a series of sub-models. Subsequently, the CO_2 capture performance can be easily modeled with process simulations, providing qualitative and quantitative knowledge for further solvent development when combined with thermodynamic analysis. However, only few reports have been found in the field of pre-combustion capture. Stavrou et al. (2014) used parameters of the perturbed-chain statistical associating fluid theory (PC-SAFT) to represent physical absorbents, where solvent parameters and process conditions were optimized simultaneously. A list of best-performing artificial solvents were obtained. Unfortunately, the effects of physical properties were not quantitatively analyzed. For post-combustion capture, more work about property analysis of the solvents can be found. The effect of the absorption heat was studied with process simulations in order to optimize the absorbents from the view of thermal performance (Hopkinson et al., 2014). Mathias (2014) created a series of artificial solvents to investigate the effects of the absorption capacity and enthalpy of absorption. More details about the impact of solvent properties were recently reported by us (Xin et al., 2020).

The aim of this research is to determine the desired phyisco-chemical properties of the absorbent for CO_2 capture by physical absorption, and the economic feasibility of DESs in particular, using rate-based process simulations of CO_2 capture by physical absorption. Firstly, a rate-based model for physical absorption is developed, where the Selexol process is used as the benchmark technology to evaluate the performance of DESs for a CO_2 capture process. Subsequently, the property and process models are constructed for a suitable DES, where in this work a mixture of decanoic acid and menthol in equal quantities has been selected. A sensitivity analysis is conducted with the recommended DES. More specifically, a hypothetical DES is simulated by altering several temperature dependent physical properties of the solvent in the simulation software to study the effects of the solvent's properties on the CO_2 absorption performance. Finally, literature review of promising DESs will be conducted based on the idealized physical property scan. The pairing of process simulation and economic evaluation of the selected DESs is done to analyze their economic feasibility for CO_2 capture, and various suggestions have been provided for viscous DESs.

METHODOLOGY

An Aspen Plus (v11.0) rate-based absorber model was developed to simulate absorption of CO_2 from a 550-MW net integrated coal gasification combined cycle (IGCC) power plant. The integrated Environmental Control Model (IECM) Version 11.2 with default settings is adopted to calculate the performance and emissions of the IGCC power plant. Medium sulfur coal (sulfur content of 2.1 wt% and a heating value of 3.08 kJ/kg) is fed to the GE Quench gasifier. To treat the coal gasification-derived syngas, the case without CO_2 capture uses a one-stage Selexol TM unit for H_2S control. For the case with CO_2 capture a water gas shift (WGS) process and physical absorption process are utilized for the selective removal of CO_2.

Process Design

At a gasification plant, fossil fuels are converted to a syngas containing mainly H_2, CO, CO_2 and H_2O. Generally, to treat the coal gasification-derived syngas, the case without CO_2 capture employed a one-stage Selexol TM unit for H_2S control. To incorporate CO_2 capture, the IGCC plant design entails two additional subsystems. The full process scheme is shown in **Figure 1**. The first additional system is a two-stage WGS reaction unit (including a high-temperature reactor and a low temperature reactor) located downstream of the gasifier quench chamber. The second sub-system is the CO_2 capture unit, which is a commercial physical absorption process, similar to the Selexol process used for sulfur (H_2S) removal in plants without CCS. The Selexol process is a proven licensed technology and is used as

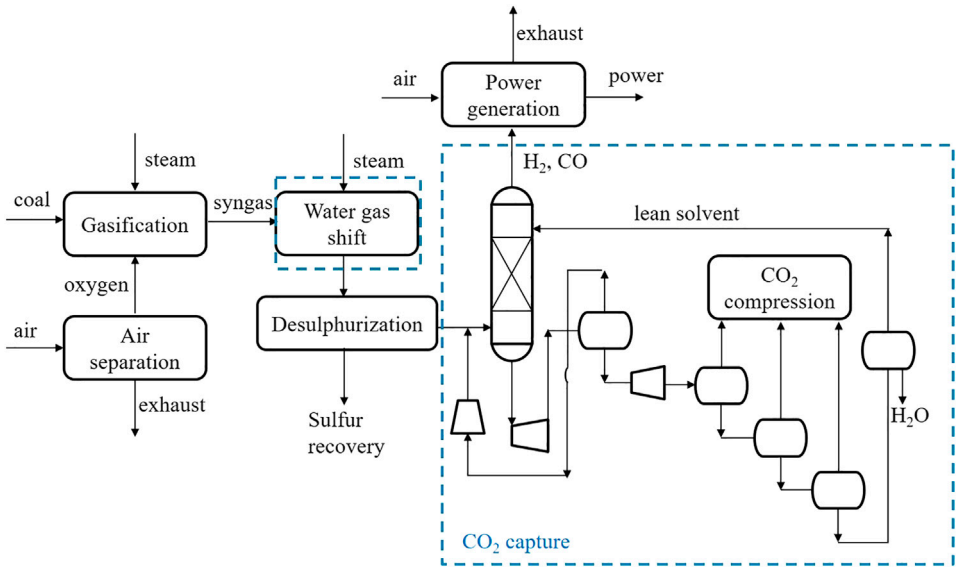

FIGURE 1 | Process flow diagram of pre-combustion CO_2 capture.

TABLE 1 | Main design assumptions.

Syngas to absorber	
Temperature [°C]	29.44
Pressure [bar]	29.58
Flow rate of gas components [kmol/h]	
N_2	209.3
CO_2	11,830
CO	442.4
H_2O	55
H_2	16,390
H_2S	2.744
CH_4	129.1
Ar	210.2
NH_3	2.091
Absorption column	
Number of stages	50
Packing type	Mellapak (structured packing)
Dimension packing	250Y
Solvent regeneration [bar]	
Pressure of flash 1	17.3
Pressure of flash 2	6.70
Pressure of flash 3	2.70
Pressure of flash 4	1.05

reference technology in this work. The process design has also been adopted for the use of DESs. The flowsheet for a DEPG-based CO_2 capture in the report by Energy Systems Division, Argonne National Laboratory (ANL) (Doctor et al., 1993) was adopted. As shown in **Figure 1** (details in **Supplementary Figure S1**), it includes an absorber for CO_2 absorption by DEPG at elevated pressure, flash tanks to release CO_2 and regenerate the solvent at several different pressure levels, and compressors and turbines to change the pressures of the streams. More specifically, for the Selexol process, the component flow rates of syngas fed to the capture plant are shown in **Table 1**. H_2 and CO_2 account for more than 96 vol%, and CO, N_2, H_2O, H_2S, CH_4, NH_3 and Ar make up the rest. After the sulfur removal, the syngas enters the bottom of the absorption tower, counter-current to the solvent flow, and the regenerated CO_2 lean solvent is fed to the top of the absorber. The CO_2 rich solvent passes the hydraulic turbine to generate electricity, followed by depressurization of the CO_2 rich solvent in four flash drums in series. The gas released from the first flash (17.3 bar) is recycled and fed back to the absorber, limiting the H_2-fraction carried away by the solvent and restoring the syngas heating value. The separated CO_2 rich gas from the second, third and fourth flash drum is compressed and cooled in a multi-stage compression system to 25°C and 130 bar for transport and storage. The last flash drum is set to 1.05 bar, ensuring the whole plant operates above atmospheric pressure. The second and third flash drums are set to 6.7 and 2.7 bar, which gives a constant expansion ratio between the two drums. More operating parameters of the CO_2 removal and compression unit can be found in the paper by Chiesa and Consonni (1999). When DESs are adopted as the absorbent, the capture process is the same as in the Selexol process. In view of the fact that CO_2, H_2 and CO make up for more than 98%, only these three components were considered in the syngas feed and other components are excluded in order to facilitate the analysis.

Thermodynamic Model

Perturbed Chain Statistical Associating Fluid Theory (PC-SAFT) equation of state (EoS) was used in the process simulation program Aspen. PC-SAFT was not only used to calculate the density, volatility and heat capacity of the absorbent, but also to describe the vapor–liquid equilibria of the solvent with different gases, while the transport property models in Aspen Plus were used to calculate transport properties.

The fluid molecules are considered as a hard chain of spherical segments in PC-SAFT, as reference for the perturbation theory, rather than the individual spherical segments (Gross and

Sadowski, 2001). More specifically, in this EOS, pure components are treated as equal-sized hard-spheres. Afterwards, the hard-spheres are bonded together and form hard-chain molecules that interact with each other in number of ways, such as by dispersion and association. All the molecular interactions can be described via the Helmholtz energy. The residual molar Helmholtz energy, defined as the difference between the total molar Helmholtz energy and that of an ideal gas at the same temperature and molar density is calculated by the sum of hard-chain, dispersion and association interactions, as expressed by **Eq. 1**.

$$a^{\mathrm{res}} = a^{\mathrm{hc}} + a^{\mathrm{disp}} + a^{\mathrm{assoc}} \quad (1)$$

A number of m_i^{seg} spherical freely jointed segments (no attractive interactions) account for the non-spherical shape of molecules and the repulsive interactions. The contribution due to dispersive interactions includes two additional parameters, namely the segment diameter (σ_i) and the dispersive energy between segments (u_i/k_B). These two parameters along with m_i^{seg} are used to fully characterize a non-associating compound. The DES was modelled as a molecule with two associating sites (2B associating scheme) in this study, which are one proton donor and one proton acceptor each. The association term introduces two additional parameters, namely the association energy ($\varepsilon^{\mathrm{AiBi}}/k_B$) and the effective association volume (κ^{AiBi}), and are used to characterize the associating interactions between unlike association sites A_i and B_i. These two parameters along with the three non-associating parameters fully describe a self-associating component. Vapor–liquid equilibria was correlated using a temperature-independent binary interaction parameter (k_{ij}), correcting the mixture dispersion energy. For more details about PC-SAFT the interested reader is referred to the works by Chen et al. (2012).

Rate-Based Model Description

This section details the flow models and mass transfer correlations used to simulate the main absorber, which are very important aspects in rate-based modeling. The rate-based model was developed based on the Selexol process. The DEPG composition for the Selexol solvent is taken from the US patent (Ameen and Furbush, 1973) and is presented in **Supplementary Table S1**. As shown in **Supplementary Tables S2, S3**, the PC-SAFT model (Aspen Technology, 2008) can describe the physicochemical properties of the Selexol solvent very well. For the Selexol process, the feed specifications and process operating conditions were set according to the report by the Argonne National Laboratory (Shi, 2014). Some key simulation results has been summarized in **Supplementary Table S4**, which were comparable with literature data. In order to investigate the effects of the flow models in the rate-based absorber, mixed, LPlug, VPlug and countercurrent models were adopted at different liquid-to-gas mass flow rate ratios (L/G ratio). The Billet and Schultes (1993) model was used for the prediction of mass transfer during CO_2 absorption. For LPlug/VPlug model, the liquid/vapor phase is considered to be in plug flow and the other phase is well mixed, while for the "mixed" model both phases are considered to be ideally mixed, and in the "countercurrent" model the liquid and vapor phases are both considered to be flowing in plug flow. The packed column was discretized into a number of segments, which models the degree of plug-flow behavior of the system (infinite segments simulates ideal plug flow, a single segment simulates an ideally stirred tank). As shown in **Supplementary Figure S2E**, with the same number of segments, very similar CO_2 recoveries are achieved with different flow models. The LPlug model is selected for the rate-based modeling afterwards to ensure easy convergence considering the poor convergence of the countercurrent model. The effects of the number of segments are investigated with the different flow models and the capture performance is summarized in the first four subfigures in **Supplementary Figure S2**. Although a larger number of segments in the absorber requires a longer computation time, nearly the same capture rates are achieved regardless of the number of segments used. The segment number has been set to 50 to save the simulation time while retaining plug flow behavior. Hanley and Chen correlations were also used to do the same analyses and the same conclusion was obtained, as shown in **Supplementary Figure S3**.

The choice of the mass transfer and interfacial area calculation model is also very important for rate-based modeling. The commonly used correlations for structured packings like the Bravo et al. (1985), Hanley and Chen (2012) and Billet and Schultes (1993) models were applied in this study for the prediction of the mass transfer rate in the absorber. These correlations were developed based on specific packing constants and different chemical systems (Razi et al., 2014). The Bravo et al. (1985) correlations were developed from cyclohexane/n-heptane and xylenes/ethylbenzene systems, whereas the Hanley and Chen (2012) correlations were developed from experiments with mixtures of alkanes. The Billet and Schultes (1993) model was validated with a large database of absorption data. The correlation equations for mass transfer and interfacial area can be found in **Supplementary Tables S5, S6**. These mass transfer models were used to model the Selexol process. As shown in **Supplementary Figure S4**, compared with the equilibrium model, the CO_2 recoveries simulated at different L/G ratios with the Bravo et al. (1985) and Billet and Schultes (1993) correlations are very similar, with an average difference of only 0.2%. This result is consistent with the results reported in the paper by Trapp et al. (2015), who performed a similar equilibrium and rate-based modelling step. It is found that the performance with the Hanley and Chen (2012) correlation for L/G ratios above 11 deviates slightly from the other two models. A relative deviation of 6.6% in CO_2 recovery is observed for the Hanley and Chen (2012) correlations at an L/G ratio of 13.78, and the deviation becomes larger at higher ratios. We conclude that all these correlations seem appropriate to describe the Selexol process and they are chosen to carry out a sensitivity analysis of solvent properties to determine the role of the solvent properties in the pre-combustion CO_2 capture process.

SENSITIVITY ANALYSIS OF SOLVENT PROPERTIES

The main objective is to investigate the effect of several different thermodynamic properties of the absorbent on the CO_2 absorption process. This was done by carrying out process

simulations with a hypothetical hydrophobic DES, which was considered as a pseudo-pure component. This hypothetical solvent is created by altering the thermodynamic properties of a low-viscous eutectic mixture of decanoic acid:menthol (deca-men) in the molar ratio of 1:1. The properties of this solvent have been listed in **Table 2**. To describe the starting material, the five pure-component PC-SAFT parameters, viz. $m_i^{seg}, \sigma_i, u_i/k_B, \varepsilon^{AiBi}/k_B$ and κ^{AiBi}, were fitted to the experimental data of density, volatility and heat capacity. VLE data of the corresponding binary systems containing the DES (CO_2 + DES, CO + DES and H_2 + DES) were correlated using the PC-SAFT equations. The binary interaction parameters k_{ij} for each binary mixture were obtained. Sub-models in Aspen were used to fit the liquid viscosity, surface tension and thermal conductivity at different temperatures. Readers can easily find the corresponding models in Aspen combined with the descriptive equations in **Table 3**. The experimental density, viscosity and vapor pressures were taken from Dietz et al. (2019). The heat capacity was determined with Differential Scanning Calorimetry (DSC) by measuring heat changes between the sample and a reference. The liquid-gas surface tension coefficient was measured with a Wilhelmy plate tensiometer. Each measurement was performed in triplicate and the average value was used. The CO_2 solubility at 298.15 and 313.15 K was studied by determining the bubble-point curve using a magnetic suspension balance (MSB, Rubotherm GmbH). The MSB and the experimental procedures are described in detail by Zubeir et al. (2014). The same instrument was used. About 2.0 g sample is loaded in the balance basket and the resolution of the mass reading is 0.01 mg. The microbalance can be tared and calibrated during measurements and the density of the gas around the sample is measured with high accuracy to correct the buoyancy effect, guaranteeing the accuracy of the measured results. The experimental surface tension, heat capacity and CO_2 solubility in deca-men (1:1) were provided in **Supplementary Tables S7, S8**. The standard deviations of surface tension and heat capacity measurements were also presented. Properties including thermal conductivity, CO and H_2 solubilities were predicted by prediction models. The thermal conductivities were predicted with the group contribution method. The conductor-like screening model for realistic solvation (COSMO-RS) method were adopted to predict the H_2 and CO solubilities in deca-men. ADF (Amsterdam Density Functional) version 2019.301 was employed to do the calculations. Decanoic acid and menthol were selected from the COSMO-RS compound database and used directly. The obtained pure-component PC-SAFT parameters, parameters for other sub-models and binary parameters for the PC-SAFT model have been summarized in **Table 3**. The absolute average relative deviation AARD (%) between the experimental data and model prediction, calculated with **Eq. 2**, is also listed in the table. All the AARDs were smaller than 6%, demonstrating good agreement of all the fitted models.

TABLE 2 | Thermodynamic properties of deca-men (1:1) at 25 °C.

Property	
Density	900.11 (kg/m^3)
Vapor pressure	1.19 (Pa)
Molar heat capacity	213.13 [J/(mol K)]
Surface tension	29.12 (mN/m)
Thermal conductivity	0.135 [Watt/(m K)]
Viscosity	20.32 (cP)
Henry's constant of CO_2	8.88 (MPa)
Henry's constant of CO	24.82 (MPa)
Henry's constant of H_2	131.66 (MPa)

$$\%\,\mathrm{AARD} = \frac{1}{n}\sum_{i=1}^{n}\left(\frac{y_i^{\exp} - y_i^{calc}}{y_i^{calc}}\right) * 100 \qquad (2)$$

By evaluating the effect of each individual property on the CO_2 recovery ratio, information is obtained regarding the optimum properties of an ideal solvent for CO_2 absorption. A one-factor-at-a-time approach was performed where each run consisted of altering one property. Each property has been evaluated with the

TABLE 3 | Model parameters for deca-men properties and the model-deviation.

Solvent property	Parameter/correlation name	Parameter value	AARD [%]
Density	$m_i^{seg}, \sigma_i, u_i/k_B$	3.891, 4.091, 315.41 K	0.27
Vapor pressure	$\varepsilon^{AiBi}/k_B, \kappa^{AiBi}$	3,364.43 K, 0.0001	5.36
Molar heat capacity			1.02
Viscosity	$\ln(\eta/\mathrm{Pa}\cdot\mathrm{s}) = A + B/T + C\ln(T/K)$	A = −164, B = 10928.3, C = 21.667	4.68
Surface tension	$\sigma/(mN/m) = C_1 + C_2(T/K) + C_3T^2 + C_4T^3$	C_1 = −53819.5, C_2 = 691.59, C_3 = −3.330, C_4 = 0.007	1.24
Thermal conductivity	$\lambda/(W/m\cdot K) = C_1 + C_2(T/K) + C_3T^2 + C_4T^3$	C_1 = −0.1395, $C_2 = -1.659\times10^{-4}$, $C_3 = -5.205\times10^{-8}$, $C_4 = 7.283\times10^{-10}$	1.03
CO_2 solubility	—	A_{ij} = 0.1613, C_{ij} = 0.0612	0.53
CO solubility	$k_{ij} = A_{ij} + C_{ij}\ln((T/°C)/25)$	A_{ij} = −0.1634, C_{ij} = 0.4352	0.12
H_2 solubility	—	A_{ij} = −0.6584, C_{ij} = 2.6139	0.23

reference case value (Run 0), and a higher and a lower value to form different hypothetical DESs. The design matrix shown in **Supplementary Table S9** was used to perform this sensitivity analysis.

Since the effects of different solvent properties on the performance of the absorption process are quite significant, for each solvent property listed in the table above, a physically realistic variation range (higher and lower values) for this property have been explored in the literature. Based on these findings, the range for the property values has been determined, and the corresponding factors with respect to the base value (Run 0) are also mentioned in the design matrix (**Supplementary Table S9**). The variation of solvent properties was carried out by adjusting the model parameters. As mentioned before, the specific heat, liquid density, vapor pressure and phase equilibrium are modelled by the PC-SAFT EoS. When one of these properties was altered, a new data set was used to regress new pure component and binary interaction parameters for each run. Thus, the temperature-dependency found through regression of the data will remain constant. The other properties have been correlated with the equations listed in **Table 3**. The first term in the right side of the equation was altered to obtain the desired property value without altering its temperature-dependency. For each hypothetical solvent thus created in the different runs described above, the Bravo et al. (1985), Billet and Schultes (1993) and Hanley and Chen (2012)models were adopted to simulate the mass transfer performance in the absorption process. Considering that the absorber configuration can affect the absorption process, three packing heights of 20, 15 and 10 m were taken into account. For Run 0 with a packing height of 20 m, the packing diameter was designed based on the criteria of a flooding point of 72%. The solvent flow rate was controlled to achieve 70% CO_2 recovery. The same solvent flow rate and absorber diameter were applied for all other runs with the other two packing heights. The results are summarized in **Tables 4–6**.

For all three rate-based correlations, the CO_2 solubility is the most important absorbent property, as expected. With doubling the CO_2 solubility, an increase of more than 20% is observed for the total CO_2 recovery. For the cases using the Bravo et al. (1985) and Billet and Schultes (1993) correlations, the effects of heat capacity, density, volatility, surface tension and thermal conductivity on the absorption process are similar. The absorption of CO_2 releases heat. A lower temperature rise along the packing is found for the solvent with a higher heat capacity, which is beneficial for the capture process. A 50% increase in heat capacity brings about an increase of 2% in CO_2 recovery. Doubling the solvent density brings about a longer residence time in the absorber, slightly intensifying the process. The effect is more pronounced, when the packing height decreases from 20 to 10 m. Due to the low volatility of DESs, the variation of vapor pressure shows a negligible effect on the CO_2 absorption performance. The effect of solvent volatility is more obvious when using the Bravo et al. (1985) correlations, where more volatile solvents vaporize more easily. Thus, more heat is taken away through solvent evaporation, resulting in a smaller temperature rise along the absorber packing and an enhanced CO_2 recovery. The surface tension and thermal conductivity hardly exert any influence on the CO_2 absorption. The solvent viscosity affects both the liquid-side mass transfer and heat transfer rates. The Billet and Schultes (1993) correlations concern both mass transfer and interfacial area, but only a very weak influence of both aspects is found. Only a small decrease of 0.12% in CO_2 recovery is found for a packing height of 10 m when the solvent viscosity is doubled. Even when the viscosity is increased 10-fold (203.2 cP at 25°C), a decrease of only 2.34% is observed. For the Bravo et al. (1985) correlations a more pronounced impact is found, where a decrease of 4.93% is calculated for an absorber packing height of 10 m when the viscosity is doubled. Because DESs can be very viscous, a sharp drop of 24.8% in the CO_2 recovery is found when the viscosity is increased further by a factor 10.

In contrast, when the Hanley and Chen (2012) correlations are applied for the rate-based absorber, the absorbent volatility and thermal conductivity have almost no influence on the absorption process. The CO_2 solubility remains obviously a very significant factor. The surface tension is included in correlations for the interfacial area, since decreasing the surface tension helps enlarging the interfacial area in gas–liquid absorbers. However, these effects are still relatively small, a 50% increase in solvent surface tension results in a 2.7% drop in CO_2 recovery (with again a packing height of 10 m). These findings are consistent with the simulation results for the other two sets of correlations. However, for the Hanley and Chen (2012) correlations the effects of the solvent viscosity are quite remarkable. The CO_2 recovery is decreased by 28.27% when the viscosity increases from 20.3 to 40.6 cP (at 25°C). The solvent temperature rises in the absorber due to the gas absorption, bringing about a decrease in liquid viscosity and enhancing the mass transfer rate. Although a higher heat capacity results in higher absorption temperature and decreases the CO_2 capacity, the solvent viscosity has such a pronounced effect in the mass transfer correlations that a lower viscosity offsets these effects. Thus, the heat capacity exerts only relatively little impact on the CO_2 recovery. Moreover, the CO_2 recovery reduces considerably for every run when the packing height is decreased from 20 to 10 m, which is also caused by the slow mass transfer rate. This also explains why the solvent density shows a large impact on the CO_2 capture. With the increase in solvent density, the contact time of the gas and the liquid is prolonged, resulting in a substantial increase in the CO_2 recovery.

Summarizing, absorbent properties such as the surface tension, thermal conductivity, heat capacity and volatility have a relatively small impact the CO_2 recovery, whereas the importance of the viscosity depends on the used correlations for mass transfer and interfacial area: the solvent viscosity strongly affects the mass transfer rate when using the Hanley and Chen (2012) correlations, while the CO_2 recovery rate shows only a small decrease with increasing solvent viscosity when the Bravo et al. (1985) correlations are adopted, and the solvent viscosity has no virtually effect on the CO_2 recovery when the Billet and Schultes (1993) correlations are used. While the CO_2 recovery is very sensitive to the solvent viscosity, the liquid density can also be an important factor, where the decrease in

TABLE 4 | Sensitivity analysis of solvent properties with Bravo et al. (1985) correlations (lean solvent flow rate of 3,495 kg/s).

Run	Property	Factor	Packing height of 20 m		Packing height of 15 m		Packing height of 10 m	
			CO_2 recovery [%]	Effect [%]	CO_2 recovery [%]	Effect [%]	CO_2 recovery [%]	Effect [%]
0	—	—	70.00	—	69.37	—	66.94	—
1	Specific heat	×1.5	72.16	2.16	71.20	1.83	68.19	1.25
2	Density	×2	70.44	0.44	70.40	1.03	69.99	3.05
3	Vapor pressure	×2	70.19	0.19	70.13	0.76	69.61	2.68
4	Surface tension	×1.5	69.99	−0.01	69.34	−0.03	66.92	−0.02
5	CO_2 solubility	×2	94.78	24.78	94.77	25.41	94.63	27.69
6	Viscosity	×2	68.79	−1.21	66.77	−2.60	62.01	−4.93
7	Thermal conductivity	×2	70.05	0.05	70.04	0.02	66.96	0.02
8	Thermal conductivity	×0.8	69.94	−0.06	69.29	−0.08	66.87	−0.06
9	Viscosity	×0.4	70.25	0.25	70.19	0.82	69.75	2.81
10	CO_2 solubility	×0.5	31.27	−38.73	31.17	−38.20	30.65	−36.28
11	Surface tension	×0.5	70.00	0.001	69.39	0.02	66.96	0.02
12	Vapor pressure	×0.1	70.03	0.03	69.75	−0.10	66.14	−0.80
13	Density	×0.8	69.55	−0.45	68.43	−0.94	65.07	−1.87
14	Specific heat	×0.5	64.32	−5.68	64.12	−5.25	63.01	−3.93

TABLE 5 | Sensitivity analysis of solvent properties with Billet and Schultes (1993) correlations (lean solvent flow rate of 3,483 kg/s).

Run	Property	Factor	Packing height of 20 m		Packing height of 15 m		Packing height of 10 m	
			CO_2 recovery [%]	Effect [%]	CO_2 recovery [%]	Effect [%]	CO_2 recovery [%]	Effect [%]
0	—	—	70.00	—	69.97	—	69.92	—
1	Specific heat	×1.5	72.32	2.32	72.30	2.33	72.24	2.31
2	Density	×2	70.23	0.23	70.22	0.24	70.19	0.27
3	Vapor pressure	×2	70.01	0.01	70.02	0.04	69.99	0.07
4	Surface tension	×1.5	69.98	−0.02	69.95	−0.02	69.86	−0.07
5	CO_2 solubility	×2	94.77	24.77	94.77	24.80	94.78	24.85
6	Viscosity	×2	69.98	−0.02	69.95	−0.02	69.80	−0.12
7	Thermal conductivity	×2	70.07	0.07	70.07	0.10	70.02	0.10
8	Thermal conductivity	×0.8	69.98	−0.02	69.94	−0.03	69.90	−0.02
9	Viscosity	×0.4	70.03	0.03	70.00	0.03	69.97	0.04
10	CO_2 solubility	×0.5	31.19	−38.81	31.18	−38.79	31.17	−38.76
11	Surface tension	×0.5	70.00	0.001	69.97	0.004	69.94	0.004
12	Vapor pressure	×0.1	70.02	0.02	69.99	0.02	69.91	−0.01
13	Density	×0.8	69.84	−0.16	69.81	−0.16	69.79	−0.22
14	Specific heat	×0.5	64.23	−5.77	64.17	−5.80	64.11	−5.81

TABLE 6 | Sensitivity analysis of solvent properties with Hanley and Chen (2012) correlations (lean solvent flow rate of 6,581 kg/s).

Run	Property	Factor	Packing height of 20 m		Packing height of 15 m		Packing height of 10 m	
			CO_2 recovery [%]	Effect [%]	CO_2 recovery [%]	Effect [%]	CO_2 recovery [%]	Effect [%]
0	—	—	69.99	—	61.32	—	47.13	—
1	Specific heat	×1.5	69.64	−0.36	60.79	−0.53	46.72	−0.41
2	Density	×2	84.92	14.93	78.88	17.56	68.13	21.00
3	Vapor pressure	×2	70.54	0.54	61.77	0.45	47.48	0.35
4	Surface tension	×1.5	67.69	−2.30	58.45	−2.87	44.43	−2.70
5	CO_2 solubility	×2	92.59	22.60	89.26	27.95	79.98	32.85
6	Viscosity	×2	41.72	−28.27	33.10	−28.22	23.27	−23.86
7	Thermal conductivity	×2	70.03	0.03	61.33	0.02	47.15	0.02
8	Thermal conductivity	×0.8	69.98	−0.01	61.31	−0.01	47.12	−0.01
9	Viscosity	×0.4	91.16	21.16	87.63	26.31	80.11	32.97
10	CO_2 solubility	×0.5	38.85	−31.14	32.86	−28.45	24.06	−23.07
11	Surface tension	×0.5	73.82	3.83	65.70	4.38	51.90	4.77
12	Vapor pressure	×0.1	66.58	−3.41	57.88	−3.44	44.51	−2.63
13	Density	×0.8	64.20	−5.79	54.22	−7.10	40.55	−6.58
14	Specific heat	×0.5	71.37	1.37	62.93	1.61	48.61	1.48

density favors a longer contact time between the gas and absorbent. In addition, equilibrium modeling was also conducted to show its difference compared with rate-based modeling. In the equilibrium model, the transport properties including surface tension, thermal conductivity and viscosity are assumed to have no impact. As confirmed in **Supplementary Table S10**, the CO_2 recovery rate stays constant with the variation of transport properties, and the density and heat capacity has only minor effects on the CO_2 capture. Overall, the CO_2 solubility is the key factor to ensure adequate CO_2 recovery, as expected, but also the liquid viscosity may be quite important to ensure a fast gas absorption rate, which should be further investigated with mass transfer rate measurements.

ECONOMIC ANALYSIS OF PROMISING DEEP EUTECTIC SOLVENTSS

Economic Analysis of Selexol Process

The CO_2 capture cost is based on the WGS process and the one-stage Selexol process. The total annual cost of 8.692 M$/year (as of 2018) for the WGS process was obtained from the Integrated Environmental Control Module (IECM) (CMU and USDOE NETL, 2020). The syngas coming out of the WGS reactor was cooled to 25°C and fed into the bottom of the absorber at a pressure of 2.958 MPa. The main assumptions for the economic analysis are presented in **Table 7**. The economic analysis has been conducted in constant money values ($2018) following the NETL methodology (Gerdes et al., 2011). Interest is added to the total overnight cost (TOC) to obtain the total capital cost. The total operating cost consists of variable (utility and solvent makeup cost) and fixed operation costs, the latter being the sum of labor, maintenance and insurance costs (**Table 8**). The methodology to calculate the TOC is presented in **Table 8**. For equipment that is accompanied with H_2, the material is selected to be stainless-steel type 316 L. The equipment costs are obtained as follows:

(1) The hydraulic turbine purchase cost was calculated according to Ogayar and Vidal (2009). As shown in **Eq. 3**, the cost (in €/kW) of a Kaplan turbine can be estimated from on the power (P, kW) and net head (H, m).

$$COST = 33236P^{-0.58338}H^{-0.113901} \quad (3)$$

(2) The Aspen Process Economic Analyzer (Version 11.0) was used to calculate the cost of other equipment in the capture plant. The total Engineering, Procurement and Construction cost (EPC) was calculated according to the Bottom-Up Approach (BUA). Lastly, contingencies and owner's cost were added up to obtain the total overnight cost (TOC).

The sum of the capital cost and operating costs (M$/year) is divided by the CO_2 capture rate (tonne/year), thus obtaining the CO_2 capture cost. The CO_2 recovery is fixed to 90%. The optimum capture cost is a trade-off between the capital cost and operating cost. As shown in **Figure 2**, where the Bravo et al. (1985) model was adopted for the rate-based modeling, with the absorber packing height decreased from 22 to 7 m, the flow rate of the lean solvent increased from 7,862 to 8,809 tonne/hr in order to reach the CO_2 recovery target. As a trade-off between the capital and operating cost, the CO_2 separation costs decreases initially and then increases when decreasing the packing height, with the lowest value of 27.22 $\$_{2018}$/tonne CO_2 at an absorber packing height of 10 m. Similar economic analysis results have been obtained for the other two rate-based models. The minimum cost of 26.66 $\$_{2018}$/tonne CO_2 is calculated for an absorber packing height of 7 m using the Billet and Schultes (1993) correlations, while using the Hanley and Chen (2012) correlations, the mass transfer rate is much slower, and the

TABLE 7 | Main assumptions for the economic analysis.

Parameter	Assumption
Base year	2018
Taxation rate	0.35
Debt interest rate	0.055
Revenue interest rate	0.12
Debt fraction	0.45
Revenue fraction	0.55
Construction payment years	3
→payment 1st year	40%
→payment 2nd year	30%
→payment 3rd year	30%
Life time	25
Operating hours	0.75 × 8,766 h
Construction years	3
Cool water T = 25 °C	0.1 $/tonne
Cool water T = 15 °C	0.2 $/tonne
Electricity	0.12 $/kWhr
Selexol price	7,200 $/tonne
DES price	7,200 $/tonne
Labor cost	28.3
Number of labors per shift	12
Maintenance cost	10% EPC
Insurance	1.5% TOC

TABLE 8 | TOC calculation methodology.

Parameter	Cost (M€)
Process equipment cost (PEC)	Sum of all equipment cost
General cost (GC)[a]	30% PEC
Total equipment cost (TEC)	PEC + GC
Direct costs as percentage of TEC	
Instrumentation (I)	15% TEC
Electrical (E)	7% TEC
Piping (P)	20% TEC
Total direct plant cost (TDPC)	TEC + I + E + P
Indirect cost (IC)[b]	14% TDPC
Engineering procurement and construction (EPC)	TDCP + IC
Contingencies and owner's cost	
Project contingency	15% EPC
Process contingency	5% EPC
Owner's cost[c]	5% EPC
Total contingencies and owner's cost (C&OC)	25% EPC
Total overnight cost (TOC)	EPC + C&OC

[a]*GC includes cost for labor, equipment integration, etc.*
[b]*IC is associated with the costs for yard improvement, buildings, sundries and engineering services.*
[C]*This cost includes pre-production costs, inventory capital, and other owner's costs.*

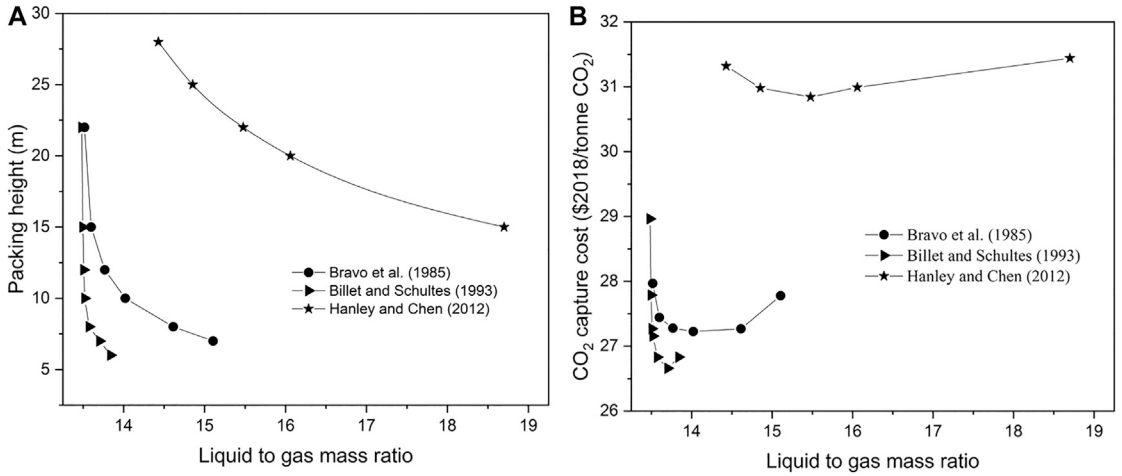

FIGURE 2 | CO_2 capture cost at different liquid to gas ratios with different rate-based model (left: packing height-L/G ratio, right: CO_2 capture cost-L/G ratio).

resulting absorber packing height needs to be much higher to allow an appropriate absorbent flow rate. With an increase in the packing height from 10 to 25 m, the demanded solvent flow rate decreases from 4,016.3 to 2,406 kg/s. The lowest cost of 30.84 $\$_{2018}$/tonne CO_2 is obtained at an absorber packing height of 22 m. Moreover, it has to be pointed out that the CO_2 compression cost takes up a large part of the CO_2 capture cost. In the CO_2 compression system CO_2 is compressed from 6.7 to 130 bar. The CO_2 compression cost is 12.14 $\$_{2018}$/tonne CO_2 in total, where the operating cost accounts for 89% of the total compression cost.

Literature Review of Deep Eutectic Solvents and Economic Analysis of CO_2 Capture by Deep Eutectic Solvents

The sensitivity analysis has shown the significance of the CO_2 solubility and liquid viscosity. In order to be able to evaluate whether the use of DESs for CO_2 absorption can be economically feasible, it is necessary to ascertain whether desired properties are realistic for a DES. Scientific papers have been reviewed in the pursuit of a DES with high CO_2 solubility, including CO_2 absorption by choline chloride based DESs (Isaifan and Amhamed, 2018), by decanoic acid based hydrophobic DESs (Zubeir et al., 2018) and by other reported DESs (Sarmad et al., 2017). In the work of Sarmad et al. (2016) several DESs have been screened in terms of their CO_2 solubility and viscosity. From this work a selection of several high CO_2 solubility DESs has been made that could enhance the CO_2 absorption process. The CO_2 solubility and viscosity of this selection is shown next to the equimolar mixture of decanoic acid and menthol and the conventional Selexol in **Figures 3A,B**, respectively. Although ethanolamine (EA) based DESs show a high CO_2 solubility and low viscosity, we did not select these since they are chemical solvents. Two diethylene glycol (DEG) based DESs were chosen to perform process simulations in view of their high CO_2 solubility. The experimental data sets are listed in **Supplementary Table S10**. The Selexol data is from the physical property model of Aspen Plus.

To build a property model for ATPPB-DEG (the mixture of allyl triphenylphosphonium bromide and diethylene glycol), the density, viscosity and CO_2 solubility of ATPPB-DEG were used to regress property parameters. The experimental data was taken from the work by Ghaedi et al. (2017a), Ghaedi et al. (2017b), Ghaedi et al. (2017c). From the sensitivity analysis results, it was concluded that the liquid surface tension, thermal conductivity, heat capacity and vapor pressure do not influence the CO_2 recovery and therefor these properties have been assumed to be the same as for deca-men. New PC-SAFT pure-component parameters and new parameters for the viscosity model were regressed. Moreover, to regress temperature depended binary parameters, data sets of CO_2 solubility at 318.15 K are assumed to be 0.81 times the CO_2 solubility at 303.15 K. The CO_2 solubility at these two temperatures were used to regress PC-SAFT binary parameters. Results of the economic the process simulations and economic analysis for ATPPB-DEG (1:4) and ATPPB-DEG (1:10) are presented in **Figures 4**, **5**, respectively.

The effect of the packed height on the capture cost for both DESs is quite similar. Almost in all cases, the operating cost accounts for more than 60% of the capture cost. When using the Billet and Schultes correlations for mass transfer, the packing height has little effect on the solvent flow rate required to achieve 90% CO_2 capture. This can also be observed from the sensitivity analysis, in which the effects of the properties are quite similar for all packed heights. For this reason, an increase in packing height would only result in a greater total capital and operating cost, due to the upscaling of the packed column. A minimum capture cost of 25.98 $\$_{2018}$/tonne CO_2 is found for ATPPB-DEG (1:4) and 25.48 $\$_{2018}$/tonne CO_2 for ATPPB-DEG (1:10), both at a packing height of 10 m. The minimum cost of 26.66 \$2018/tonne CO_2 was calculated for the Selexol process. Thus, both selected DESs present an economic advantage over the Selexol solvent. In contrast to the Billet and Schultes correlations, the packing height does have a significant effect on the absorber performance in the Bravo et al. correlations. A

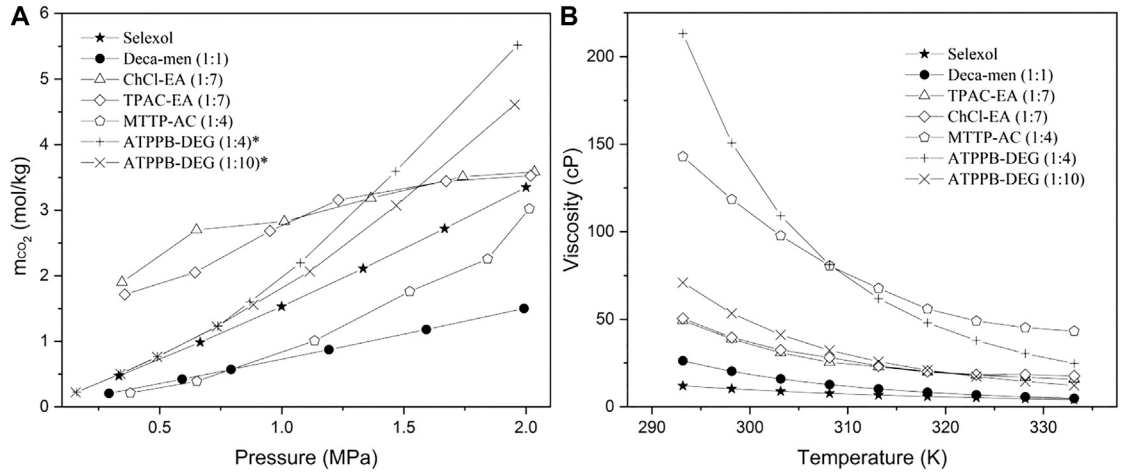

FIGURE 3 | (A): CO_2 solubility as a function of pressure at 298.15 K (*absorption temperature of 303.15 K) and **(B)**: viscosity as a function of temperature at atmospheric pressure of Selexol and the DESs Deca-men (1:1), ChCl-EA (1:7), TPAC-EA (1:7), TPAC-EA (1:7), MTTP-AC (1:4), ATPPB-DEG (1:4), ATPPB-DEG (1:10). ChCl, choline chloride; TPAC, tetrapropylammonium chloride, MTTP; methyltriphenyl phosphonium bromide; ATPPB, allyl triphenylphosphonium bromide; EA, ethanolamine; AC, acetic acid and DEG, diethylene glycol. The ratio in brackets, the mole ratio of hydrogen bond donor and acceptor.

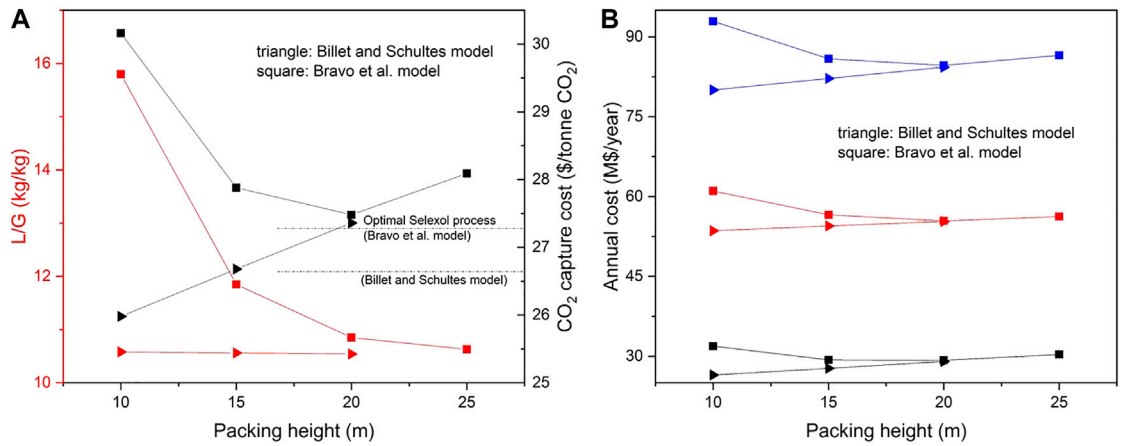

FIGURE 4 | (A) The variation of L/G ratio along with the packing height for ATPPB-DEG (1:4). Red lines and symbols refer to the left red axis, black lines and symbols refer to the right black axis; **(B)** The variation of CO_2 capture cost along with the packing height for ATPPB-DEG (1:4). Black/red/blue samples and symbols refer to capital/operating/total annual cost, respectively.

packing height of 20 m is found to be the optimum regarding the capture cost. Another increase in packing height would not have any more significant impact on the solvent requirement and thus results in an increase in capture cost. A minimum capture cost of 27.48 $\$_{2018}$/tonne CO_2 is found for ATPPB-DEG (1:4) and 26.90 $\$_{2018}$/tonne CO_2 for ATPPB-DEG (1:10), both at a packing height of 20 m. Optimum cost of 27.22 $\$_{2018}$/tonne CO_2 was calculated for the Selexol process with the same mass transfer model. The process costs based on ATPPB-DEG can be on similar level than based on Selexol when the Bravo et al. correlations can be applied. In the Hanley and Chen correlations, the only correlations where the liquid viscosity shows a significant effect on the CO_2 capture rate, either very large solvent flow rates or higher absorber packing heights are required to achieve the same CO_2 recovery due to the slow gas diffusion rate in viscous solvent. Due to the high viscosity of ATPPB-DEG (1:4), a solvent flowrate of 10,118.26 kg/s could only achieve 74.97% CO_2 capture ratio but results in a very high capture cost of 72.49 $\$_{2018}$/tonne CO_2. The viscosity of ATPPB-DEG (1:10) is about one third of ATPPB-DEG (1:4) at absorption temperatures. With an increase in packing height from 20 to 30 m, the L/G ratio is decreased from 67.74 to 40.45, bringing about a decrease in operating cost. Although the absorber size is increased, the size of other equipment is smaller, resulting in a decrease in the capital cost and an obvious drop in capture cost. Considering the lowest cost of 30.84 $\$_{2018}$/tonne CO_2 was obtained for Selexol solvent, at current operating conditions, the use of ATPPB-DEG

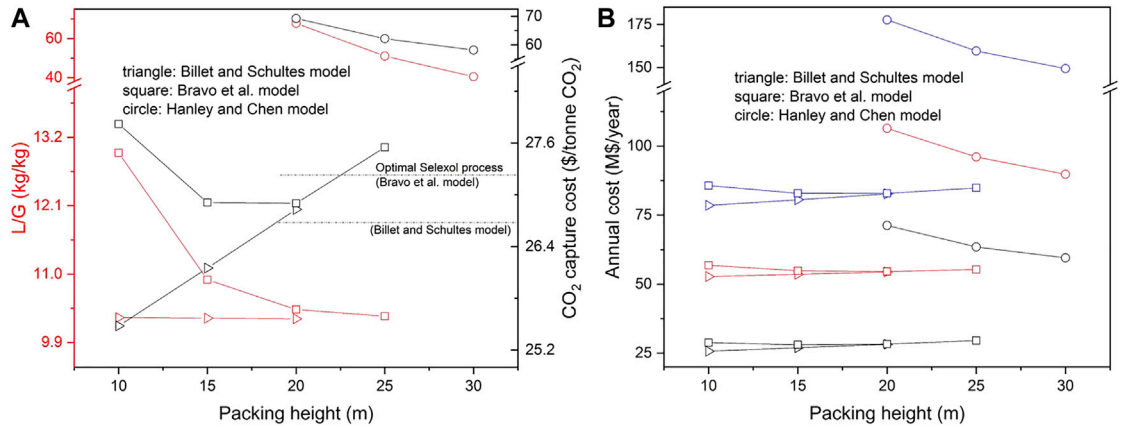

FIGURE 5 | (A) The variation of L/G ratio along with the packing height for ATPPB-DEG (1:10). Red lines and symbols refer to the left red axis, black lines and symbols refer to the right black axis; **(B)** The variation of CO_2 capture cost along with the packing height for ATPPB-DEG (1:10). Black/red/blue samples and symbols refer to capital/operating/total annual cost, respectively.

(1:4) and ATPPB-DEG (1:10) does not seem economically feasible, according to the correlations by Hanley and Chen.

PROSPECTS TO APPLY DEEP EUTECTIC SOLVENTS IN PRE-COMBUSTION CAPTURE

The importance of the liquid viscosity is different in the three rate-based models. In this section, we assume viscosity is very important for the absorption process and provide suggestions including a higher absorption temperature and absorber packing height. Among the three mass transfer correlations, the viscosity exerts significant impact on the absorption process only in the Hanley and Chen model. Thus only the Hanley and Chen model was adopted for the rate-based model and ATPPB-DEG (1:10) was selected for the analysis. It is shown in **Supplementary Table S12** that the solvent viscosity is decreased by 50% when the temperature is increased from 298.15 to 318.15 K. As shown in **Figure 6**, due to the enhancement of the mass transfer rate, the required liquid-to-gas ratio decreases from 40.45 to 17.95 for a packing height of 30 m. The capture cost is above 60 \$/tonne CO_2 for the investigated cases for the absorption temperature of 298.15 K. The sharp decrease in solvent flow rate brings about a large reduction in solvent purchase cost and equipment size, and the CO_2 capture cost is reduced to 42.68 \$/tonne CO_2 when the absorption temperature is raised to 313.15 K. A further increase in temperature results in a small change in solvent demand and capture cost, related to the limited CO_2 solubility at higher temperatures. To make a highly viscous solvent economically feasible, a high CO_2 solubility at a relatively high temperature seems very promising. Moreover, as already presented in **Figure 5**, the slow gas diffusion rate in the viscous ATPPB-DEG demands a larger amount of solvent or a higher packing height. A steady decrease in capture cost is found for larger packing heights. But the influence of the packing height is less pronounced, especially at higher absorption temperatures.

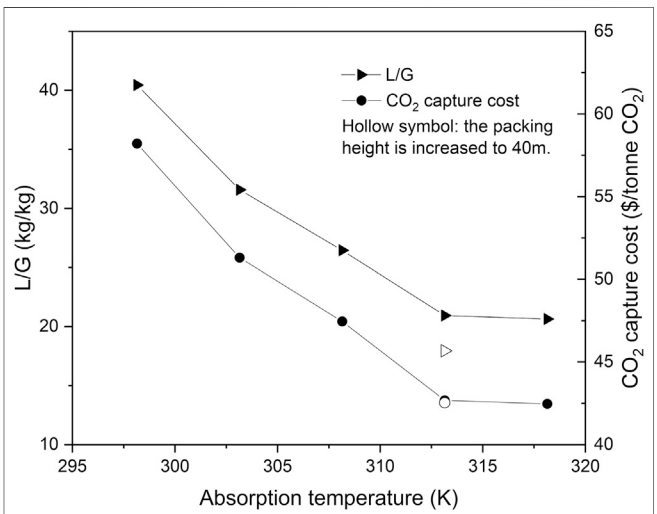

FIGURE 6 | L/G ratio and CO_2 capture cost at different absorption temperatures.

When the absorber packing height is enlarged to 40 m at 313.15 K, despite the decrease in L/G ratio from 20.93 to 17.95, the capture cost only decreases from 42.68 to 42.54 $\$_{2018}$/tonne CO_2. More details about the analysis results can be found in **Supplementary Table S13**.

It should be pointed out that the mass transfer models are built on a variety of experimental bases and theoretical hypothesis. And they have different accuracy, limitations and ranges of suitability for different applications. More mass transfer models (Wang et al., 2005) should be embedded in Aspen to repeat the procedures in this research. Experimental work needs to be conducted to measure the rate of gas-liquid mass transfer in viscous solvents to help improving the correlations for process design and better evaluating the feasibility of using DESs for pre-combustion CO_2 capture. It should also be emphasized that DESs

are sustainable solvents, especially the green DESs prepared from natural ingredients (Dai et al., 2013). Nowadays green hydrophobic DESs becomes a hot research area (Florindo et al., 2019). An advanced capture process with much higher absorption temperature is suggested for hydrophobic absorbents (Koronaios et al., 2016). According to the process modeling results from National Energy Technology Laboratory (Netl and Parsons, 2010), if CO_2 can be selectively removed from the stream (250°C and 5.5 MPa) coming out of the WGS reactor using physical solvents with little or no cooling and water remains in the gas phase, then the combustion of H_2–H_2O gas mixture in the gas turbine system will result in an increase of 2–3 percentage point in IGCC plant thermal efficiency. It is interesting to adopt hydrophobic DESs for high temperature absorption processes. Moreover, for traditional solvents like Selexol, the tradition production method of glycol etherification takes place in a solution of strong base (Zupancic and Sopcic, 1979). The impact on the environment during the production of the solvents should also be assessed to make a fairer comparison. Moreover, more efforts need to be undertaken to develop more DESs with high CO2 solubility.

CONCLUSION

A rate-based modeling approach was adopted to evaluate the effectiveness of various pre-combustion CO_2 capture strategies based on DES absorption. The conventional Selexol process was used as the benchmark technology. The effects of the flow model in the absorber were investigated, and as a result, the liquid phase absorbent was modelled as plug flow, while the gas phase was modelled as a fully mixed phase in the developed process model. Bravo et al. (1985), Billet and Schultes (1993) and Hanley and Chen (2012) correlations were adopted for the rate-based models. For the Selexol process, the first two correlations obtained similar simulation results compared with the equilibrium model. Deviations were observed when using the Hanley and Chen (2012) correlations at high L/G ratios. The property and process models were built for an often-used DES for CO_2 absorption, namely an even mixture of decanoic acid and menthol. Sensitivity analyses of various physical properties were conducted with these three rate-based models. The CO_2 solubility is important in all analysis cases, as expected, whereas surface tension, thermal conductivity, heat capacity and volatility have only a minor influence on the process efficiency when using DESs for pre-combustion capture. However, the significance of the liquid viscosity on the absorption process is still unclear. The solvent viscosity strongly affects the mass transfer rate when employing the Hanley and Chen (2012) correlations, but it plays only a minor role when using the other two rate-based models. Based on the sensitivity analysis results, ATPPB-DEG (1:4) and ATPPB-DEG (1:10) were selected from literature screening, both bearing favorable properties. The pairing of process simulation and economic evaluation of the selected DESs was done to analyze their economic feasibility for precombustion CO_2 capture. The optimum capture cost is a trade-off between the capital cost and operating cost. For the benchmark Selexol process, the optimum capture cost is 27.22, 26.66 and 30.84 $\$_{2018}$/tonne CO_2 for the Bravo et al. (1985), Billet and Schultes (1993) and Hanley and Chen (2012) correlations, respectively. ATPPB-DEG (1:4) can outperform Selexol, according to two of the three studied mass transfer correlations. However, when the liquid viscosity strongly affects the mass transfer rate, the conventional Selexol process is still the more economical option. More studies are required to elucidate the role of the liquid viscosity on the mass transfer rates. In addition, a higher absorption temperature and absorber packing height can help reducing the capture cost for viscous DESs. More efforts need to be paid to develop new DESs with low viscosity and high CO_2 solubility, or DESs that possess high CO_2 solubility at high temperatures.

DATA AVAILABILITY STATEMENT

The original contributions presented in the study are included in the article/**Supplementary Material**, further inquiries can be directed to the corresponding author.

AUTHOR CONTRIBUTIONS

MA and KX: conceptualization and methodology. KX and MH: investigation and simulations. KX: writing—original draft preparation. IR and MA: writing-review and editing. IR and KX: visualization. IR and MA: supervision.

ACKNOWLEDGMENTS

KX is grateful to the China Scholarship Council (CSC) for a Ph.D. Scholarship.

SUPPLEMENTARY MATERIAL

The Supplementary Material for this article can be found online at: https://www.frontiersin.org/articles/10.3389/fenrg.2020.573267/full#supplementary-material.

REFERENCES

Ameen, J., and Furbush, S. A. (1973). *Solvent composition useful in acid gas removal from gas mixtures*. U.S. Patent and Trademark Office, U.S. Patent No 3737392.

Aspen Technology (2008). *Aspen polymers model of the CO_2 capture process by DEPG*. New York, NY: Aspen Technology.

Ban, Z. H., Keong, L. K., and Shariff, A. M. (2014). Physical absorption of CO_2 capture: a review. *Adv. Mater. Res.* 917, 134–143. doi:10.4028/www.scientific.net/AMR.917.134

Billet, R., and Schultes, M. (1993). Predicting mass transfer in packed columns. *Chem. Eng. Technol.* 16, 1–9. doi:10.1002/ceat.270160102

Bravo, J. L., Rocha, J. A., and Fair, J. R. (1985). Mass transfer in gauze packings. *Hydrocarb. Process.* 64 (1), 91–95.

Burr, B., and Lyddon, L. (2008). "A comparison of physical solvents for acid gas removal," in Proceedings of the 87th GPA annual convention, Grapevine, TX, March 2–5, 2008: Bryan Research & Engineering, Inc.

Chen, Y., Mutelet, F., and Jaubert, J. N. (2012). Modeling the solubility of carbon dioxide in imidazolium-based ionic liquids with the PC-SAFT equation of state. *J. Phys. Chem. B* 116, 14375. doi:10.1021/jp309944t

Chiesa, P., and Consonni, S. (1999). Shift reactors and physical absorption for low-CO_2 emission IGCCs. *J. Eng. Gas Turb. Power* 121, 295. doi:10.1115/1.2817120

CMU, and USDOE NETL (2020). *Integrated environmental control model*, Pittsburgh, PA: Carnegie Mellon University.

Dai, Y., Van Spronsen, J., Witkamp, G. J., Verpoorte, R., and Choi, Y. H. (2013). Natural deep eutectic solvents as new potential media for green technology. *Anal. Chim. Acta.* 766, 61. doi:10.1016/j.aca.2012.12.019

Dietz, C. H. J. T., Creemers, J. T., Meuleman, M. A., Held, C., Sadowski, G., Van Sint Annaland, M., et al. (2019). Determination of the total vapor pressure of hydrophobic deep eutectic solvents: experiments and perturbed-chain statistical associating fluid theory modeling. *ACS Sustain. Chem. Eng.* 7, 4047. doi:10.1021/acssuschemeng.8b05449

Doctor, R. D., Molburg, J. C., Thimmapuram, P., Berry, G. F., Livengood, C. D., and Johnson, R. A. (1993). Gasification combined cycle: carbon dioxide recovery, transport, and disposal. *Energy Convers. Manag.* 44, 67–108. doi:10.1016/0196-8904(93)90060-N

Florindo, C., Branco, L. C., and Marrucho, I. M. (2019). Quest for green-solvent design: from hydrophilic to hydrophobic (deep) eutectic solvents. *ChemSusChem* 12, 1549–1559. doi:10.1002/cssc.201900147

García, G., Aparicio, S., Ullah, R., and Atilhan, M. (2015). Deep eutectic solvents: physicochemical properties and gas separation applications. *Energ. Fuel.* 29, 2616–2644. doi:10.1021/ef5028873

Gerdes, K., Summers, W. M., and Wimer, J. (2011). Cost estimation methodology for NETL assessments of power plant performance. DOE/NETL-2011/1455, 26, 2011. Available at: http://www.netl.doe.gov/File Library/research/energy analysis/publications/QGESSNETLCostEstMethod.pdf.

Ghaedi, H., Ayoub, M., Sufian, S., Lal, B., and Shariff, A. M. (2017a). Measurement and correlation of physicochemical properties of phosphonium-based deep eutectic solvents at several temperatures (293.15 K-343.15 K) for CO_2 capture. *J. Chem. Thermodyn.* 113, 41. doi:10.1016/j.jct.2017.05.020

Ghaedi, H., Ayoub, M., Sufian, S., Shariff, A. M., Hailegiorgis, S. M., and Khan, S. N. (2017b). CO_2 capture with the help of Phosphonium-based deep eutectic solvents. *J. Mol. Liq.* 243, 564–571. doi:10.1016/j.molliq.2017.08.046

Ghaedi, H., Ayoub, M., Sufian, S., Shariff, A. M., and Lal, B. (2017c). The study on temperature dependence of viscosity and surface tension of several Phosphonium-based deep eutectic solvents. *J. Mol. Liq.* 241, 500. doi:10.1016/j.molliq.2017.06.024

Gross, J., and Sadowski, G. (2001). Perturbed-chain SAFT: an equation of state based on a perturbation theory for chain molecules. *Ind. Eng. Chem. Res.* 40, 1244. doi:10.1021/ie0003887

Hanley, B., and Chen, C.-C. (2012). New mass-transfer correlations for packed towers. *AIChE J.* 58, 132–152. doi:10.1002/aic.12574

Hopkinson, D., Luebke, D., Li, Z., and Chen, S. (2014). Solvent optimization of conventional absorption processes for CO_2 capture from postcombustion flue gases. *Ind. Eng. Chem. Res.* 53, 7149. doi:10.1021/ie403869y

Isaifan, R. J., and Amhamed, A. (2018). Review on carbon dioxide absorption by choline chloride/urea deep eutectic solvents. *Adv. Chem.* 2018, 1–6. doi:10.1155/2018/2675659

Koronaios, P., Stevenson, C., Warman, S., Enick, R., and Luebke, D. (2016). Thermally stable silicone solvents for the selective absorption of CO_2 from warm gas streams that also contain H_2 and H_2O. *Energ. Fuel.* 30, 5901. doi:10.1021/acs.energyfuels.6b00140

Mathias, P. M. (2014). Some examples of the contribution of applied thermodynamics to Post-Combustion CO_2-Capture technology. *Fluid Phase Equil.* 362, 102–107. doi:10.1016/j.fluid.2013.09.016

Netland Parsons (2010). Current and future technologies for gasification-based power generation volume 2: a pathway study focused on carbon capture advanced power systems R&D using bituminous coal. Available at: www.netl.doe.gov (Accessed July 22, 2020).

Ogayar, B., and Vidal, P. G. (2009). Cost determination of the electro-mechanical equipment of a small hydro-power plant. *Renew. Energy* 34, 6. doi:10.1016/j.renene.2008.04.039

Razi, N., Svendsen, H. F., and Bolland, O. (2014). Assessment of mass transfer correlations in rate-based modeling of a large-scale CO_2 capture with MEA. *Int. J. Greenh. Gas Control* 26, 93–108. doi:10.1016/j.ijggc.2014.04.019

Sarmad, S., Mikkola, J. P., and Ji, X. (2017). Carbon dioxide capture with ionic liquids and deep eutectic solvents: a new generation of sorbents. *ChemSusChem* 10, 324. doi:10.1002/cssc.201600987

Sarmad, S., Xie, Y., Mikkola, J. P., and Ji, X. (2016). Screening of deep eutectic solvents (DESs) as green CO_2 sorbents: from solubility to viscosity. *New J. Chem.* 41, 290. doi:10.1039/c6nj03140d

Shi, F. (2014). *Reactor and process design in sustainable energy technology*. 1st Eedn. Oxford, UK: Elsevier. doi:10.1016/C2012-0-00576-5

Stavrou, M., Lampe, M., Bardow, A., and Gross, J. (2014). Continuous molecular targeting-computer-aided molecular design (CoMT-CAMD) for simultaneous process and solvent design for CO_2Capture. *Ind. Eng. Chem. Res.* 53, 18029–18041. doi:10.1021/ie502924h

Trapp, C., de Servi, C., Casella, F., Bardow, A., and Colonna, P. (2015). Dynamic modelling and validation of pre-combustion CO_2 absorption based on a pilot plant at the Buggenum IGCC power station. *Int. J. Greenh. Gas Control* 36, 13. doi:10.1016/j.ijggc.2015.02.005

Wang, G. Q., Yuan, X. G., and Yu, K. T. (2005). Review of mass-transfer correlations for packed columns. *Ind. Eng. Chem. Res.* 44, 8715. doi:10.1021/ie050017w

Xin, K., Gallucci, F., and Annaland, M. V. S. (2020). Optimization of solvent properties for post-combustion CO_2 capture using process simulation. *Int. J. Greenh. Gas Control* 99, 103080. doi:10.1016/j.ijggc.2020.103080

Zubeir, L. F., Lacroix, M. H. M., and Kroon, M. C. (2014). Low transition temperature mixtures as innovative and sustainable CO_2 capture solvents. *J. Phys. Chem. B* 118, 14429. doi:10.1021/jp5089004

Zubeir, L. F., Van Osch, D. J. G. P., Rocha, M. A. A., Banat, F., and Kroon, M. C. (2018). Carbon dioxide solubilities in decanoic acid-based hydrophobic deep eutectic solvents. *J. Chem. Eng. Data* 63, 913. doi:10.1021/acs.jced.7b00534

Zupancic, B. G., and Sopcic, M. (1979). ChemInform abstract: glycol etherification IN a solid-liquid two-phase system. *Chem. Informationsd.* 10, (21). doi:10.1002/chin.197921166

Conflict of Interest: The authors declare that the research was conducted in the absence of any commercial or financial relationships that could be construed as a potential conflict of interest.